

# Dynamic Analysis of Nonlinear Models with Infinite Extension by Boundary Elements

Delfim Soares Jr., and Webe J. Mansur

**Abstract**—The Time-Domain Boundary Element Method (TD-BEM) is a well known numerical technique that handles quite properly dynamic analyses considering infinite dimension media. However, when these analyses are also related to nonlinear behavior, very complex numerical procedures arise considering the TD-BEM, which may turn its application prohibitive. In order to avoid this drawback and model nonlinear infinite media, the present work couples two BEM formulations, aiming to achieve the best of two worlds. In this context, the regions expected to behave nonlinearly are discretized by the Domain Boundary Element Method (D-BEM), which has a simpler mathematical formulation but is unable to deal with infinite domain analyses; the TD-BEM is employed as in the sense of an effective non-reflective boundary. An iterative procedure is considered for the coupling of the TD-BEM and D-BEM, which is based on a relaxed renewal of the variables at the common interfaces. Elastoplastic models are focused and different time-steps are allowed to be considered by each BEM formulation in the coupled analysis.

**Keywords**—Boundary Element Method, Dynamic Elastoplastic Analysis, Iterative Coupling, Multiple Time-Steps.

## I. INTRODUCTION

IN this paper two boundary element formulations, namely the so-called D-BEM (Domain Boundary Element Method) and the TD-BEM (Time-Domain Boundary Element Method), are employed in order to perform 2D non-linear elastodynamic analyses. The D-BEM formulation employs the static fundamental solution (Kelvin fundamental solution) and keeps, in the BEM integral equations, the domain integral related to the inertial terms, i.e., the domain integral related to the acceleration [1], [2]. As a consequence, in order to perform dynamic analyses, the entire domain has to be discretized and time marching schemes, similar to those employed by Finite Element Method, may be adopted in order to advance in time. TD-BEM formulations, on the other hand, employ time-dependent fundamental solutions [3], [4]. The fulfilment of the radiation condition by the fundamental solution turns this formulation very suitable for performing infinite domain analysis, since there are no reflected waves from infinity.

Due to the characteristics of the two BEM formulations mentioned above, it looks natural and straightforward to employ, in a non-linear elastodynamic analysis, the D-BEM

formulation for the part of the domain in which inelastic behaviour is expected to occur and the TD-BEM formulation for the part of the domain that behaves elastically (along the text, these sub-domains will be referred to simply as D-BEM sub-domain and TD-BEM sub-domain, respectively). In an infinite domain analysis, the interface between the non-linear and the linear domains, that is, between the D-BEM sub-domain and the TD-BEM sub-domain, can be interpreted as an efficient non-reflecting boundary.

It is important to mention that in BEM dynamic analyses the correct choice of the time-step length plays a fundamental role [3]. As the time-step lengths required by the D-BEM to produce reliable results are usually smaller than those required by the TD-BEM, special time-marching procedures are employed, which turns out to be very easy to implement in an iterative coupling approach [5]. The proposed final algorithm is very effective, as demonstrated by the examples presented at the end of this paper.

## II. BOUNDARY ELEMENT FORMULATIONS

### A. Time-Domain Boundary Element Method

The integral equation based on dynamic fundamental solutions that solves the elastodynamic model in focus is given by:

$$c_{ik}(\xi) u_k(\xi, t) = \iint_{\Gamma} u_{ik}^*(X, t; \xi, \tau) \tau_k(X, \tau) d\Gamma(X) d\tau + \iint_{\Gamma} \tau_{ik}^*(X, t; \xi, \tau) u_k(X, \tau) d\Gamma(X) d\tau + s(X, t; \xi, \tau), \quad (1)$$

where  $\Gamma$  is the boundary of the body,  $c_{ik}(\xi)$  depends on the geometry, and the terms  $u_{ik}^*(X, t; \xi, \tau)$  and  $\tau_{ik}^*(X, t; \xi, \tau)$  represent the dynamic fundamental displacement and traction, respectively.  $X$  is the field point,  $\xi$  is the source point, and  $s(X, t; \xi, \tau)$  stands for possible domain integrals contributions (initial conditions or/and body forces). Adopting the following space-time approximations for the variables of the model ( $v_k$  stands for  $u_k$  or  $\tau_k$ ;  $\eta$  and  $\phi$  are space and time interpolation functions, respectively, related to a boundary node  $j$  and a discrete time  $m$ ):

$$v_k(X, t) = \sum_{j=1}^J \sum_{m=1}^M \phi_j^m(t) \eta_v^j(X) v_{kj}^m, \quad (2)$$

D. Soares, Jr., is with the Federal University of Juiz de Fora, Structural Engineering Department, CEP 36036-330, Juiz de Fora, MG, Brazil (e-mail: delfim.soares@ufjf.edu.br).

W.J. Mansur is with the Federal University of Rio de Janeiro, Department of Civil Engineering, CP 68506, CEP 21945-970, Rio de Janeiro, RJ, Brazil (e-mail: webe@coc.ufrrj.br).

the following system of equations can be obtained:

$$\mathbf{C}\mathbf{U}^n = \mathbf{G}^1\mathbf{T}^n - \mathbf{H}^1\mathbf{U}^n + \sum_{m=1}^{n-1} (\mathbf{G}^{n-m+1}\mathbf{T}^m - \mathbf{H}^{n-m+1}\mathbf{U}^m) + \mathbf{S}^n, \quad (3)$$

where  $\mathbf{C}$ ,  $\mathbf{G}$  and  $\mathbf{H}$  are influence matrices;  $\mathbf{S}^n$  is related to domain integrals and  $\mathbf{U}^n$  and  $\mathbf{T}^n$  are displacement and traction vectors, respectively, at the discrete time  $n$ . After introducing the boundary conditions of the model, the system of equations (3) can be solved for displacements and tractions, at each time  $t_n$ . For more details concerning the present formulation, the reader is referred to [4].

#### B. Domain Boundary Element Method

The integral equations based on static fundamental solutions that solves the dynamic elastoplastic model in focus (displacements and stresses) are given by:

$$\begin{aligned} c_{ik}(\xi) u_k(\xi, t) = & \int_{\Gamma} u_{ik}^*(X; \xi) \tau_k(X, t) d\Gamma(X) + \\ & - \int_{\Gamma} \tau_{ik}^*(X; \xi) u_k(X, t) d\Gamma(X) + \int_{\Omega} \varepsilon_{ikj}^*(X; \xi) \sigma_{jl}^P(X, t) d\Omega(X) + \\ & - \int_{\Omega} u_{ik}^*(X; \xi) \rho \{ \ddot{u}_k(X, t) - b_k(X, t) \} d\Omega(X), \end{aligned} \quad (4)$$

$$\begin{aligned} \sigma_{ik}(\xi, t) = & \int_{\Gamma} u_{ikj}^*(X; \xi) \tau_j(X, t) d\Gamma(X) + \\ & - \int_{\Gamma} \tau_{ikj}^*(X; \xi) u_j(X, t) d\Gamma(X) + \int_{\Omega} \varepsilon_{ikjl}^*(X; \xi) \sigma_{jl}^P(X, t) d\Omega(X) + \\ & - \int_{\Omega} u_{ikj}^*(X; \xi) \rho \{ \ddot{u}_j(X, t) - b_j(X, t) \} d\Omega(X) + g_{ik}(X, t), \end{aligned} \quad (5)$$

where the terms  $u_{ik}^*(X; \xi)$ ,  $\tau_{ik}^*(X; \xi)$  and  $\varepsilon_{ikj}^*(X; \xi)$ , as well as  $u_{ikj}^*(X; \xi)$ ,  $\tau_{ikj}^*(X; \xi)$  and  $\varepsilon_{ikjl}^*(X; \xi)$ , represent the elastostatic fundamental solutions.  $b_j(X, t)$  stands for body forces terms,  $\rho$  is the mass density of the model, and  $\ddot{u}_j(X, t)$  stands for accelerations.  $\sigma_{jl}^P(X, t)$  represents the “initial” (plastic) stress components and the free term  $g_{ik}(\sigma_{jl}^P(X, t))$  is due to the derivative of the initial stress domain integral.  $\Omega$  stands for the domain of the body. Adopting the following generic space approximation for the variables of the model ( $j$  stands for boundary element nodes or cell nodes; dual reciprocity formulations are also possible):

$$v_k(X, t) = \sum_{j=1}^J \eta_v^j(X) v_{kj}(t), \quad (6)$$

the following system of equations can be obtained, after suitable algebraic operations:

$$\mathbf{C}\mathbf{U}^n = \mathbf{G}\mathbf{T}^n - \mathbf{H}\mathbf{U}^n + \mathbf{W}\mathbf{O}^n - \mathbf{M}\ddot{\mathbf{U}}^n + \mathbf{S}^n, \quad (7)$$

$$\mathbf{O}^n = \mathbf{G}'\mathbf{T}^n - \mathbf{H}'\mathbf{U}^n + \mathbf{W}'\mathbf{O}^n - \mathbf{M}'\ddot{\mathbf{U}}^n + \mathbf{S}'^n, \quad (8)$$

where matrices  $\mathbf{H}$ ,  $\mathbf{G}$ ,  $\mathbf{H}'$  and  $\mathbf{G}'$  correspond to the boundary integrals, whereas matrices  $\mathbf{M}$ ,  $\mathbf{W}$ ,  $\mathbf{M}'$  and  $\mathbf{W}'$  correspond to the inertial and initial stress domain integrals (the free term depicted in equation (5) is dealt with in  $\mathbf{W}'$ ). Vector  $\mathbf{O}^n$  stands for the stress nodal values.  $\mathbf{S}^n$  and  $\mathbf{S}'^n$  are the vectors related to body force terms and  $\mathbf{U}^n$  and  $\mathbf{T}^n$  are displacement and traction vectors, respectively, at time step  $n$ . To solve the system of equations (7)-(8) the boundary conditions of the model have to be considered and a time-integration scheme has to be adopted (the present work adopts the Houbolt method [6]). Moreover, an iterative algorithm must be considered in order to properly evaluate the problem stress state (elastoplastic model). The present work adopts the Newton-Raphson scheme in order to deal with non-linear effects. After considering the above-mentioned procedures, the system of equations (7)-(8) can be solved for displacements, tractions and stresses, at each time step. For more details concerning the present formulation, the reader is referred to [1].

### III. COUPLING PROCEDURES

In the current section, the iterative coupling of the BE formulations previously presented is considered. Some important procedures with which the coupled numerical solution becomes more efficient, accurate and stable are firstly described. These procedures are, namely: (i) adoption of a relaxation parameter  $\alpha$  in order to ensure or/and speed up the convergence of the iterative coupling process; (ii) adoption of time interpolation/extrapolation procedures in order to consider independent time discretizations for the different BE formulations.

In the iterative coupling procedure, a relaxation parameter  $\alpha$  is introduced, which relates the recent BEM results ( $^{(k+\alpha)}\mathbf{V}$ ) with the results of the previous iterative step ( $^{(k)}\mathbf{V}$ ) and the final results ( $^{(k+1)}\mathbf{V}$ ) at the current iterative step. Considering a generic variable  $\mathbf{V}$ , the adoption of the relaxation parameter  $\alpha$  can be described as follows:

$$^{(k+1)}\mathbf{V} = (\alpha)^{k+\alpha}\mathbf{V} + (1-\alpha)^{k}\mathbf{V}. \quad (9)$$

In order to consider different time-steps (namely  $_{TD}\Delta t$  and  $_{D}\Delta t$ , where the left-side subscripts  $_{TD}$  and  $_{D}$  stand for the TD-BEM and the D-BEM, respectively) in each sub-domain, interpolation/extrapolation procedures along time may be considered. In the present work, the interpolation/extrapolation procedures are based on the BEM time interpolation functions (e.g., piecewise constant  $\phi_r(t)$  and linear  $\phi_u(t)$ ), as depicted by Fig. 1.

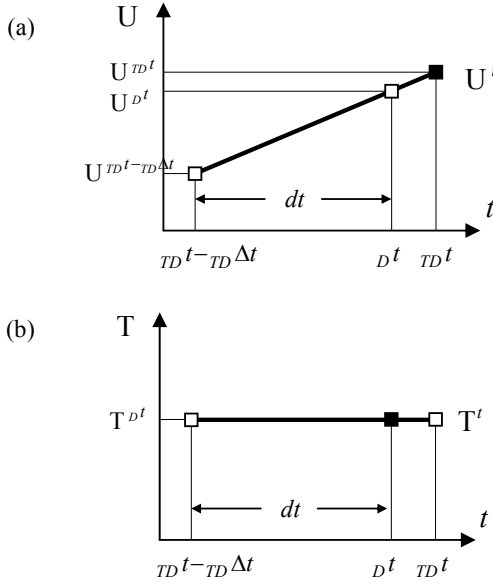


Fig. 1 Time interpolation/extrapolation procedures: (a) time extrapolation:  $U^{TD^t} = U^{D^t} (TD\Delta t / dt) + U^{TD^t-TD\Delta t} (1 - TD\Delta t / dt)$ ;

(b) time interpolation:  $T^{D^t} = T^{TD^t}$

The boundary conditions (equilibrium and continuity conditions, respectively) at coupling interfaces are given by:

$${}_D \mathbf{T}^t + {}_{TD} \mathbf{T}^t = \mathbf{0}, \quad (10)$$

$${}_D \mathbf{U}^t - {}_{TD} \mathbf{U}^t = \mathbf{0}. \quad (11)$$

In the iterative coupling of the previously described BEM formulations, at the common interfaces, natural boundary conditions are prescribed for the sub-domains modeled by the D-BEM and essential boundary conditions are prescribed for the sub-domains modeled by the TD-BEM. The displacements evaluated at the sub-domains modeled by the D-BEM are used to obtain the interface displacements (prescribed interface boundary condition) for the sub-domains modeled by the TD-BEM (11); the tractions evaluated at the sub-domains modeled by the TD-BEM are used to obtain the tractions (prescribed interface boundary condition) for the sub-domains modeled by the D-BEM (10). Concisely, each sub-domain is solved separately ( ${}_D \mathbf{U}^t$  and  ${}_{TD} \mathbf{T}^t$  are evaluated at each iterative step) and the interface relations  ${}_D \mathbf{U}^t \rightarrow {}_{TD} \mathbf{U}^t$  and  ${}_{TD} \mathbf{T}^t \rightarrow {}_D \mathbf{T}^t$  are iteratively considered until convergence is achieved. A basic algorithm solution for the adopted iterative coupling is shown on Table I.

TABLE I  
ITERATIVE COUPLING ALGORITHM

- (1) **Initial calculations:**
  - (1.1) Time steps for each sub-domain are selected ( ${}_{TD} \Delta t$ ,  ${}_D \Delta t$ ) and initial time attribution is adopted:  ${}_{TD} t = {}_{TD} \Delta t$  and  ${}_D t = 0$ .
  - (1.2) BEM standard initial calculations are considered (influence matrices  $\mathbf{G}^1$ ,  $\mathbf{H}^1$  etc.) and initial prescribed values are chosen at the common interface surfaces (e.g.,  ${}^{(0)}_D \mathbf{T} = \mathbf{0}$ ).
- (2) **Time-step loop:**
  - (2.1) Beginning of evaluations at each time step: update  ${}_D t = {}_D t + {}_D \Delta t$ . If  ${}_D t > {}_{TD} t$  then: update  ${}_{TD} t = {}_{TD} t + {}_{TD} \Delta t$  and evaluate convolution and body term vectors.
  - (2.2) **Iterative loop:**
    - (2.2.1) Solve D-BEM: obtain  ${}^{(k+\alpha)}_D \mathbf{U}^{D^t}$ .
    - (2.2.2)  ${}^{(k+1)}_D \mathbf{U}^{D^t} = (\alpha) {}^{(k+\alpha)}_D \mathbf{U}^{D^t} + (1-\alpha) {}^{(k)}_D \mathbf{U}^{D^t}$ .
    - (2.2.3) From  ${}^{(k+1)}_D \mathbf{U}^{D^t}$  obtain  ${}^{(k+1)}_{TD} \mathbf{U}^{D^t}$  (Eq.11).
    - (2.2.4) From  ${}^{(k+1)}_{TD} \mathbf{U}^{D^t}$  obtain  ${}^{(k+1)}_{TD} \mathbf{U}^{TD^t}$  (time extrapolation).
    - (2.2.5) Solve TD-BEM: obtain  ${}^{(k+1)}_{TD} \mathbf{T}^{TD^t}$ .
    - (2.2.6) From  ${}^{(k+1)}_{TD} \mathbf{T}^{TD^t}$  obtain  ${}^{(k+1)}_{TD} \mathbf{T}^{D^t}$  (time interpolation).
    - (2.2.7) From  ${}^{(k+1)}_{TD} \mathbf{T}^{D^t}$  obtain  ${}^{(k+1)}_D \mathbf{T}^{D^t}$  (Eq.10).
    - (2.2.8) Check for convergence.
  - (2.3) Updating (and printing) of D-BEM results. If  ${}_D t + {}_D \Delta t > {}_{TD} t$  then: updating (and printing) of TD-BEM results.
  - (2.4) Go to the next time step until the analysis is finished.
- (3) **End of calculations**

#### IV. NUMERICAL APPLICATIONS

Two examples are considered here. The first one deals with a nonlinear cantilever beam (finite-domain problem), and the second one is concerned with a nonlinear circular cavity (infinite-domain problem). Results related to the proposed TD-BEM/D-BEM coupling algorithm are compared with other numerical results, showing the good accuracy of the proposed methodology.

##### A. Cantilever Beam

This example consists of a cantilever beam submitted to a Heaviside type forcing load. Fig. 2(a) shows the boundary conditions, geometry and selected internal point A. Fig. 2(b) shows the coupled TD-BEM/D-BEM mesh adopted: 64 linear boundary elements of equal length are employed (32 boundary elements for TD-BEM and 32 boundary elements for D-BEM), as well as 128 linear triangular integration cells (D-BEM formulation).

The adopted time-steps are:  ${}_{TD} \Delta t = 0.015s$  and  ${}_D \Delta t = 0.005s$ .

The physical properties of the model are given by:  $\nu = 0.0$  (Poisson's ratio);  $E = 100 \text{ N/m}^2$  (Young's modulus);  $\rho = 1.5 \text{ kg/m}^3$  (mass density); and  $\sigma_0 = 0.1 \text{ N/m}^2$  (uniaxial yield stress — von Mises yield criterion).

The geometry of the beam is defined by  $a = 2\text{m}$  and  $b = 1\text{m}$ .

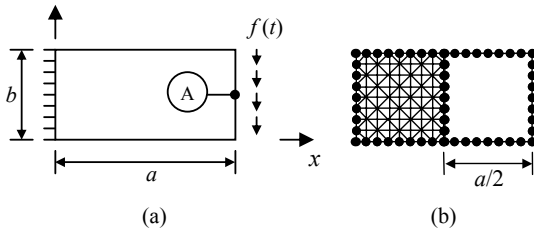


Fig. 2 Cantilever beam: (a) geometry, boundary conditions and selected boundary point; (b) coupled mesh

Fig. 3 depicts time-history results for the vertical displacements at point A considering the coupled TD-BEM/D-BEM formulation, as well as results provided by standard TD-BEM and D-BEM acting alone (with analogous time and space discretization). Fig. 4 indicates the average number of iterative steps per time-step necessary for converge, taking into account different relaxation parameter values.

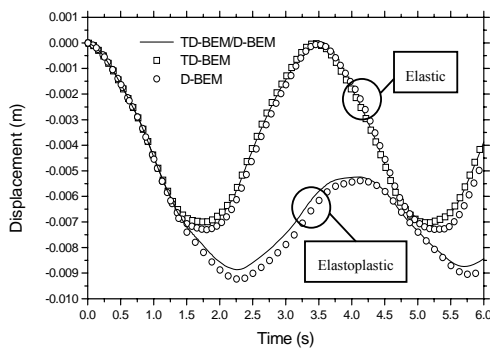


Fig. 3 Vertical displacement time-history results considering coupled TD-BEM/D-BEM, TD-BEM, and D-BEM analyses

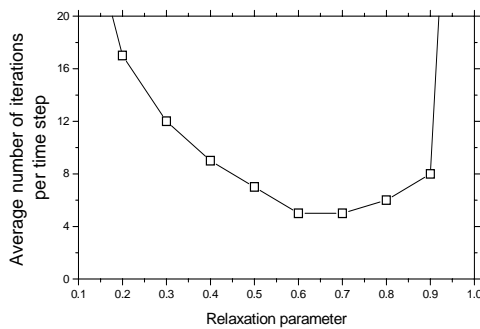


Fig. 4 Average number of iterations per time-step for convergence, taking into account different relaxation parameter values

As one can observe, good results are obtained by the coupled methodology and convergence is achieved quite rapidly once appropriate relaxation parameters are considered.

### B. Circular Cavity

This plane strain problem consists of a circular cavity under a uniform internal pressure suddenly applied and kept constant in time. A sketch of the model is shown in Fig. 5(a). The boundary element and internal cell discretization is depicted in Fig. 5(b): 46 linear boundary elements are employed in the TD-BEM/D-BEM coupled analysis (20 boundary elements for TD-BEM and 26 boundary elements for D-BEM), as well as 270 linear triangular cells (D-BEM formulation). In the present analysis the double symmetry of the problem is taken into account. An interesting feature of the boundary element formulation is that symmetric bodies under symmetric loads can be analysed without discretization of the symmetry axes. This can be accomplished by an automatic condensation process, which integrates over reflected elements and performs the assemblage of the final matrices in reduced size [7].

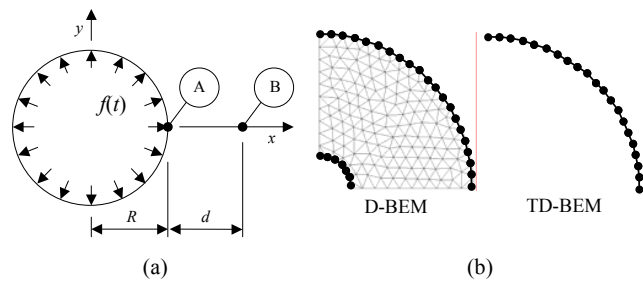


Fig. 5 Circular cavity: (a) geometry, boundary conditions and selected boundary node and internal point; (b) coupled mesh

The physical properties of the model are:  $\nu = 0.2308$ ,  $E = 6.5277 \cdot 10^8 \text{ N/m}^2$ , and  $\rho = 1.804 \cdot 10^3 \text{ kg/m}^3$ . A perfectly plastic material obeying the Mohr-Coulomb yield criterion is assumed: cohesion  $= 4.8263 \cdot 10^6 \text{ N/m}^2$ , internal friction angle  $= 30^\circ$ . The geometry of the problem is defined by:  $R = 3.048 \text{ m}$ , and  $d = 3.658 \text{ m}$ . The time discretization adopted is given by:  $_{TD}\Delta t = _D\Delta t = 0.2 \text{ s}$  (since, in this case, multiple wave reflexions do not occur, a larger range of time-steps can be considered in the analysis, allowing the same time-step to be adopted for both formulations).

Time histories of radial ( $\sigma_R$ ) and circumferential ( $\sigma_C$ ) stress components, at boundary node A ( $x = R$  and  $y = 0$ ) and internal point B ( $x = R + d$  and  $y = 0$ ), are depicted in Figs. 6 and 7. Displacement time history is plotted in Fig. 8. The linear TD-BEM/D-BEM results are compared with results related to the TD-BEM formulation, obtained by adopting a richer mesh of 12 linear boundary elements to model the 1/4 of the cavity (once again the symmetry of the problem is considered). Stresses at internal points for the TD-BEM analysis were computed employing complex algebra [8]. As one can observe, good agreement is obtained between the TD-BEM and TD-BEM/D-BEM formulations (Figs. 6, 7 and 8 are also in good agreement with results obtained by Chow and Koenig [9]).

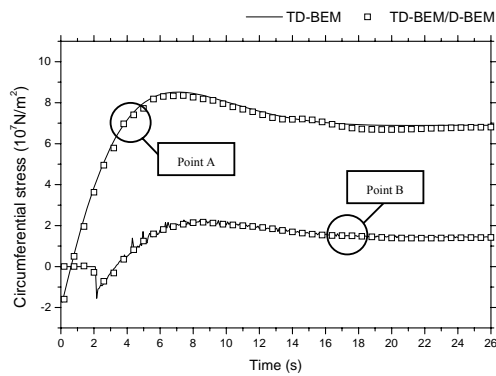
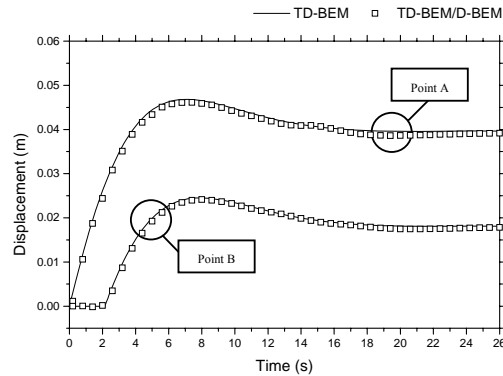
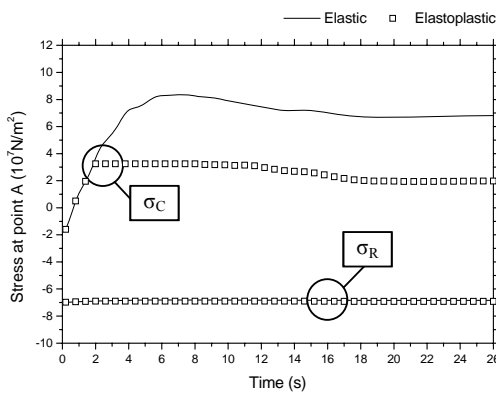


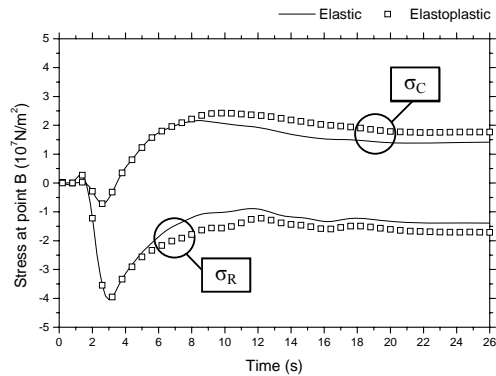
Fig. 6 Linear circumferential stresses: TD-BEM solution and coupled TD-BEM/D-BEM solution



(a)



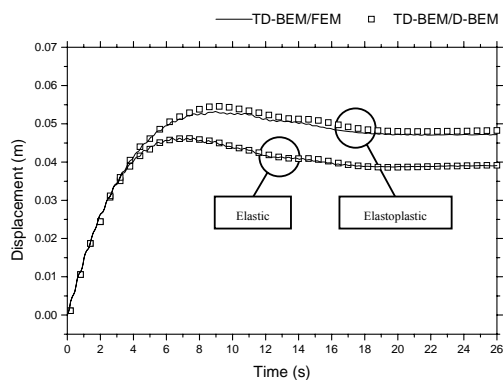
(a)



(b)

Fig. 7 Linear and nonlinear stresses for the coupled TD-BEM/D-BEM solution: (a) stresses at point A; (b) stresses at point B

In Fig. 8(b), the TD-BEM/D-BEM displacement time-history at point A is plotted, considering linear and nonlinear analyses. Results concerning a TD-BEM/FEM coupled analysis [5] are also plotted in Fig. 8(b), for comparison: once again, good agreement can be observed.



(b)

Fig. 8 Radial displacement considering TD-BEM, coupled TD-BEM/D-BEM, and coupled TD-BEM/FEM solutions: (a) linear results; (b) linear and nonlinear results at point A

## V. CONCLUSION

The methodology for the solution of non-linear dynamic problems presented in this work proved to be very efficient, as it makes use of the main advantages of two different BEM formulations: finite domains with non-linear behaviour can be modelled by the D-BEM formulation, which is very simple, and infinite (finite) domains with linear behaviour can be modelled by the TD-BEM formulation. Due to the characteristics of the latter, it is possible to solve infinite domain problems very appropriately, since no artificial boundaries are introduced in the analysis (this eliminates the possible influence of spurious reflected waves). Besides, iterative coupling at common interfaces does not demand a high computational cost and can be easily implemented in a computer code.

## ACKNOWLEDGMENT

The financial support by CNPq (Conselho Nacional de Desenvolvimento Científico e Tecnológico) and FAPEMIG (Fundação de Amparo à Pesquisa do Estado de Minas Gerais) is greatly acknowledged.

## REFERENCES

- [1] J.A.M. Carrer, and J.C.F. Telles, "A Boundary Element Formulation to Solve Transient Dynamic Elastoplastic Problems," *Computers and Structures*, vol. 45, pp. 707-713, 1992.
- [2] J.A.M. Carrer, and W.J.Mansur, "Alternative Time-Marching Schemes for Elastodynamic Analysis with the Domain Boundary Element Method Formulation," *Computational Mechanics*, vol. 34, pp. 387-399, 2004.
- [3] W.J.Mansur, *A Time-stepping Technique to Solve Wave Propagation Problems Using the Boundary Element Method*. Ph.D. Thesis, University of Southampton, England, 1983.
- [4] J. Dominguez, *Boundary Elements in Dynamics*. Southampton and Boston: Computational Mechanics Publications, 1993.
- [5] D. Soares Jr., O. von Estorff, and W.J. Mansur, "Iterative Coupling of BEM and FEM for Nonlinear Dynamic Analysis," *Computational Mechanics*, vol. 34, pp. 67-73, 2004.
- [6] J.C. Houbolt, "A Recurrence Matrix Solution for the Dynamic Response of Elastic Aircraft," *Journal of the Aeronautical Sciences*, vol. 17, pp. 540-550, 1950.
- [7] J.C.F. Telles, *The Boundary Element Method Applied to Inelastic Problems*, Lecture Notes in Engineering, vol.1. Berlin, New York, Heidelberg, Tokyo: Springer-Verlag, 1983.
- [8] D. Soares Jr., J.A.M. Carrer, J.C.F. Telles, and W.J. Mansur, "Time-domain BEM Formulation: Two Approaches for the Computation of Stress and Velocity," *Computational Mechanics*, vol. 30, pp. 38-47, 2002.
- [9] P.C. Chow, and H.A. Koenig, "A Unified Approach to Cylindrical and Spherical Elastic Waves by Method of Characteristics," *Transactions of the ASME, Journal of Applied Mechanics*, vol. 33, pp. 159-167, 1966.